IEEE Access
Multidisciplinary | Rapid Review | Open Access Journal

Received May 29, 2020, accepted June 22, 2020, date of publication June 30, 2020, date of current version August 11, 2020.

Digital Object Identifier 10.1109/ACCESS.2020.3006046

Highly Precise Birefringence Demodulation to Overcome the Sensing Limitation From the Free Spectral Range on the Fiber Lyot Filter

WEI LI, TIANTIAN RUAN, MIN XIA, AND LI XIA
School of Optical and Electronic Information, Huazhong University of Science and Technology, Wuhan 430074, China
Corresponding author: Min Xia (xiamin@hust.edu.cn)

This work was supported by NSFC under Grant 61775065.

ABSTRACT A high precision demodulation method based on least squares fitting for expanding the temperature measurement range of the fiber Lyot filter has been proposed and experimentally demonstrated. And a compact reflective Lyot filter has also been proposed to verify this method. The filter consists of a polarizer and a section of polarization maintaining fiber (PMF) coated with a gold film at the end. The birefringence of the PMF can be obtained through the least squares method, so that the temperature measurement range is not limited to the free spectral range (FSR) of the periodic interference spectrum. Experimental results show that the proposed method can extend the measurement range by 5.5 times compared to the dip wavelength tracking method. And the demodulation fluctuation of the birefringence is within 10^{-7}.

INDEX TERMS Demodulation, fiber Lyot filter, polarization interference, temperature measurement.

I. INTRODUCTION

The research on optic fiber temperature sensors with large measurement range and high precision characteristics is of great significance in the fields of aerospace, healthcare and industrial production [1], [2]. Up to now, various fiber structures with a large dynamic measurement range have been proposed, such as Mach-Zehnder (MZ) interferometers [3], [4], two peanut-shaped structures [5], and fiber gratings [6], [7]. However, relatively low sensitivity of less than 0.5 nm/°C is the main constraint. Therefore, research on sensitivity-enhanced temperature sensors have attracted great attention. One of the methods is to combine high sensitivity refractive index sensors with thermosensitive materials. For instance, a liquid-filled photonic crystal fiber achieves sensitivity of up to 53.4 nm/°C in the 1500-1600 nm region. However, the temperature measurement range of this structure is only from 34.0 to 35.5 °C [8]. Another common approach is to increase the sensitivity through the Vernier effect. For example, the cascaded structure of a Sagnac loop and a Fabry-Perot cavity can achieve an ultra-high sensitivity of −29nm/°C, while the relatively narrow measurement range is from 42 to 44 °C [9]. In short, the trade-off between high sensitivity and large-scale exists in most fiber optic temperature sensors. In order to solve this problem, a special fiber with two sensing mechanisms is proposed to realize large-scale and high-precision sensing simultaneously [10]. Among the two mechanisms, the lower sensitivity anti-resonance enables a large measurement range, while the higher sensitivity MZ interference is used to ensure high precision. However, for the high sensitivity MZ interference, the sensitivity may vary over different temperature ranges, which causes inconvenience to the actual measurement calibration. In addition, it is noted that the above-mentioned sensors are mostly demodulated by the dip wavelength tracking method, which makes the measurement range of the interference type sensor limited to the free spectral range (FSR) and the observation window.

The Lyot filter, with polarization interference, consisting of a birefringent cavity and two polarizers, has been extensively studied [11]. At present, a variety of Lyot filters have been developed for spectral imaging [12], [13], optical communication [14], laser tuning [15], [16] and fiber sensing [17]–[20]. For temperature sensing applications, most of them are demodulated by the dip wavelength tracking method, so the measurement range is limited by FSR of the interference spectrum. In fact, for the Lyot filter, the change in the interference spectrum during temperature detection is mainly caused by the change in the birefringence which is

The associate editor coordinating the review of this manuscript and approving it for publication was Muguang Wang.

highly sensitive to temperature [20]. Therefore, the absolute demodulation of the birefringence for temperature measurement can be free from the limitation of the FSR, thereby expanding the temperature measurement range.

The least squares curve fitting method [21], as an effective method for accurately evaluating parameters in the model, has been widely used in spectroscopy and sensing applications. Specifically, it is mostly applied to fiber Brillouin distributed sensing parameter extraction [22] and fiber Fabry-Perot cavity length evaluation [23], but rarely used for Lyot filter birefringence demodulation.

In our work, we propose a high precision demodulation method for expanding the temperature measurement range of the fiber Lyot filter. Specifically, the least squares method is utilized to demodulate the birefringence of the polarization maintaining fiber (PMF) in the filter, so that the temperature demodulation range is not limited by the FSR of the interference spectrum, thereby expanding the temperature measurement range by 5.5 times. In addition, a new reflective Lyot filter composed of a polarizer and a PMF coated with gold film has also been proposed to make the temperature sensor more compact and practical.

II. OPERATION PRINCIPLE

As shown in Fig. 1(a), the transmissive Lyot filter is constructed by splicing a section of high-birefringence PANDA PMF (1550-XP) between two polarizers. The polarizer1 is used to convert the broadband light into linearly polarized light, which is incident into the PMF and then resolved into two light beams propagating along the fast- and slow-axis of the PMF. Due to the birefringence existing in the PMF, there is a phase difference between the two light beams, which is calculated by:

$$\Delta\varphi = \frac{2\pi BL_{PMF}}{\lambda} \tag{1}$$

where LPMF and B are the length and the birefringence of the PMF, respectively; λ is the operating wavelength. Finally, the two polarized light beams meet at the polarizer2, then the polarization interference occurs, and can be described as:

$$T(\lambda) = C_1(\lambda) + C_2(\lambda)\cos(\frac{2\pi BL_{PMF}}{\lambda}) \tag{2}$$

where C1(λ) represents the background light intensity and C2(λ) indicates the interference spectrum amplitude.

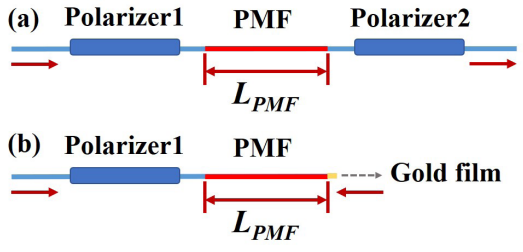

FIGURE 1. Schematic diagram of the (a) transmissive and (b) reflective fiber Lyot filter.

Fig. 1 (b) shows the schematic diagram of the new reflective Lyot filter. The end face of the PMF is coated with a highly durable gold film to increase the reflectivity. The two polarized beams with relative phase differences mentioned above are reflected by the gold film and meet at the polarizer1 to form the polarization interference. Since the polarized beam passes through the PMF twice, this is equivalent to doubling the cavity length [24]. Therefore, the polarization interference of the reflective Lyot filter can be described as:

$$R(\lambda) = C_1(\lambda) + C_2(\lambda)\cos(\frac{4\pi BL_{PMF}}{\lambda}) \tag{3}$$

Then, the polarization interference spectrum is finally detected by the spectrometer, and the sampling interval is adjusted to 0.1 nm. It should be noted that, the initial power of the light source needs to be subtracted during spectrometer detection to eliminate the influence of the uneven light source on the interference spectrum. Therefore, $C_1(\lambda)$ and $C_2(\lambda)$ can be written as C_1 and C_2, respectively. And the spectrum was fitted using the least-squares method. The specific demodulation process is to calculate a set of best (C_1, C_2, LPMF, B) to minimize the Sum of the Squares for Error (SSE), which can be expressed as:

$$SSE_1 = \sum_1^N \left[T_i - C_1 - C_2\cos(\frac{2\pi BL_{PMF}}{\lambda_i})\right]^2 \tag{4}$$

and

$$SSE_2 = \sum_1^N \left[R_i - C_1 - C_2\cos(\frac{4\pi BL_{PMF}}{\lambda_i})\right]^2 \tag{5}$$

where the λ_i is the sampling wavelength; $T(\lambda_i)$ and $R(\lambda_i)$ are the intensity at different wavelength, corresponding to the transmissive and reflective Lyot filter respectively.

In fact, after the filter is prepared, the length LPMF of the PMF is determined. Furthermore, a group of initial values (C_1, C_2, B) also needs to be set before the actual calculation to improve the demodulation efficiency. The initial C_1 and C_2 can be calculated based on the maximum and minimum values of the detected light intensity. The initial B can be obtained by Fast Fourier Transform (FFT) method. Specifically, the spatial frequency f is first obtained by applying FFT to the interference spectrum, and then the initial B is calculated according to the following formula:

$$B_0 = \frac{\lambda^2 \mathrm{f}}{L_{PMF}} \tag{6}$$

For a reflective Lyot filter, LPMF needs to be doubled in Eq.6. After setting the initial value, the B is fine-tuned to minimize the SSE, and then the optimal B can be obtained. Specifically, in the process of adjusting the B value, the step value is set to 10^{-9}. In the wavelength range from 1520 to 1610 nm, the spectrum of the transmissive Lyot filter with B value of 4.45683×10^{-4} is fitted by the least squares method mentioned above, and the change of calculated SSE with B values in the fitting process is shown in Fig. 2. It can be seen

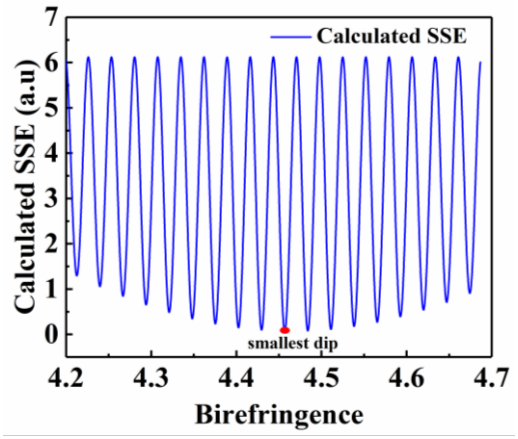

FIGURE 2. The calculated SSE changes with birefringence B when the actual B is 4.456843×10^{-4}.

that as the value of B changes, there will be multiple dips in the SSE, and the optimal B corresponds to the smallest dip. The rest of the dips indicate that the actual spectrum and the fitted spectrum partially match, but the interference order is not consistent in the spectral range. Therefore, the algorithm can distinguish the order of interference. In other words, when the amount of spectral shift is an integer multiple of FSR, the algorithm can still distinguish the interference spectrum. So, when the amount of spectral shift is greater than FSR, different optimal B values can still be demodulated, which makes the measurement of B not affected by the periodicity of the spectrum, thereby expanding the measurement range in subsequent experiments.

III. EXPERIMENTAL MEASUREMENT AND DISCUSSION

A. TRANSMISSIVE FIBER LYOT FILTER

In order to verify the ability of the proposed demodulation method to expand the measurement range by experiments, the temperature measurement system using the transmissive Lyot filter is proposed, as shown in Fig. 3. In this configuration, the length of the PMF is 28 cm. The broad-band source (BBS) with wavelength range from 1520nm to 1610nm is emitted into the polarizer1. The interference spectrum output from the polarizer 2 is received by the optical spectrum analyzer (OSA, AQ6370C) with a resolution of 0.1 nm. The commercial fiber polarization controller (PC) is used to adjust the state of the polarized light launched into the PMF from the polarizer1, thereby obtaining an optimum angle between the direction of polarized light and the two polarization axes within the PMF. In general, the optimum

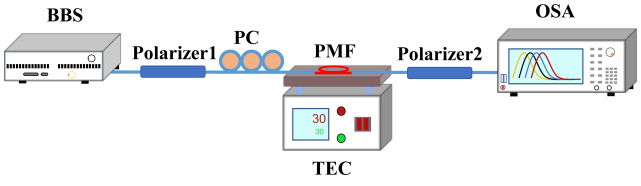

FIGURE 3. Experimental setup of the transmissive fiber Lyot filter for temperature measurement.

angle is 45 degrees, so that polarization interference with high fringe contrast can be achieved. However, it should be noted that, we can pre-set the angle between the directions of the two polarizers and the polarization axes of the PMF to 45 degrees, so that the PC is not essential for this temperature sensor in practical applications.

First, we demodulate the transmissive fiber Lyot filter based on the dip wavelength tracking method. The full width at half maxima (FWHM) of each dip is less than 0.1 nm and the dip depth is higher than 20 dB, observed from the inset in the Fig. 4(a). The ambient temperature is increased from 25°C to 76°C controlled by a Thermoelectric Cooler with the resolution of 0.2°C (TEC). As shown in Fig. 4(a), as the temperature increases, the wavelength of the dips shift to the shorter-wavelength direction, namely "blue shift". And the interference spectrum at different temperatures ranging from 25 to 35 ° C is described in the inset. The selected wavelength dip at 1577.9 nm shifts to 1561.8nm, corresponding to the wavelength variation of 16.1 nm. It is noted that the FSR of the spectrum is 18.4 nm, which is slightly larger than the shift variation, which allows the temperature to be distinguished by the dip wavelength in the range of 25 °C to 35 °C. In addition, the relationship between the dip wavelength and temperature is also demonstrated. After linear fitting, the temperature sensitivity is 1.61 nm/°C.

Then the proposed demodulation method is applied to the transmissive fiber Lyot filter. The change in the filter birefringence as a function of the ambient temperature is shown in Fig. 4 (b). The temperature sensitivity is 4.7×10^{-7}/°C, and the corresponding wavelength shift sensitivity of 1.62nm/°C is basically consistent with the above measurement result, which is calculated by:

$$\frac{\partial \lambda}{\partial T} = \lambda \frac{\partial B}{B \partial T} \tag{7}$$

where the T is the ambient temperature. In addition, the stability of the filter and demodulation method has also been tested. The demodulation results of repeated 10 experiments within 50 minutes is illustrated in Fig. 4(c), the maximum and minimum values of the demodulated B are 4.48163×10^{-4} and 4.48063×10^{-4}, respectively. Therefore, the demodulation fluctuation is within 10^{-7}, and the corresponding temperature fluctuation is about 0.2 °C, which is exactly the accuracy of the TEC. Therefore, the birefringence demodulation fluctuation is due to fluctuations in ambient temperature. If a higher precision TEC is used, higher demodulation stability may be obtained.

B. REFLECTIVE FIBER LYOT FILTER

In order to make the sensor more compact and practical, a novel reflective fiber Lyot filter is prepared. A gold film of approximately 50 nm thick was applied to the end of the 15 cm long PMF and tested for temperature using the system shown in Fig. 5. The reflectivity of metal film is higher than 90%, this will not lead to the FP interference dips in the reflection spectrum. In this case, a circulator is used to

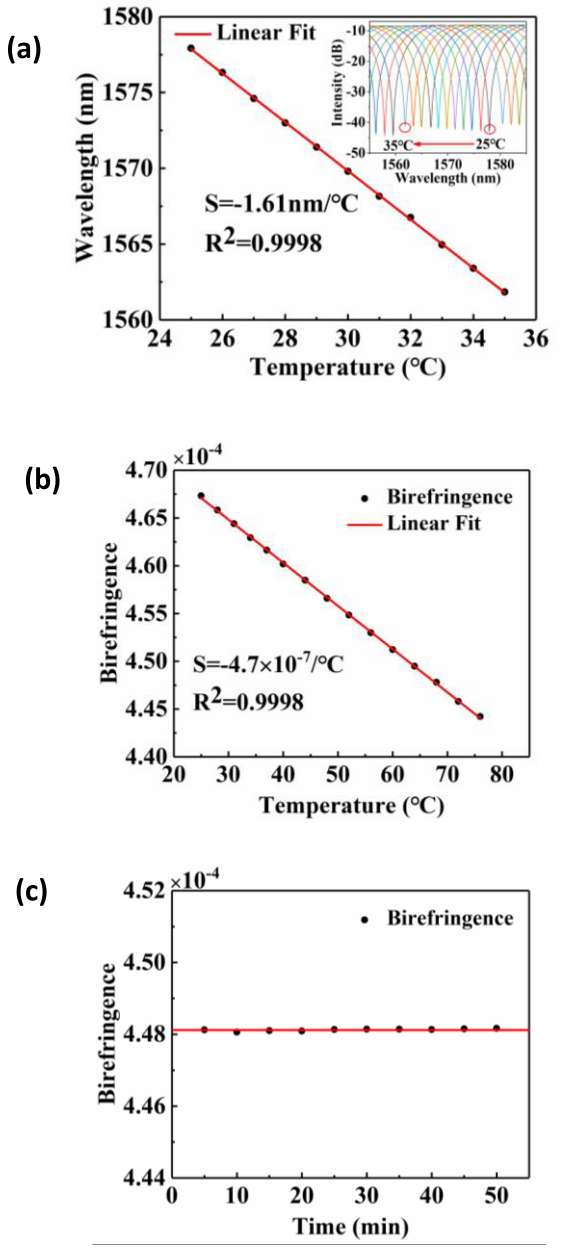

FIGURE 4. (a) Dip wavelength changes with temperature. The inset is the spectra at different temperatures of the transmissive fiber Lyot filter; (b) Birefringence of the transmissive fiber Lyot filter versus temperature; (c) Demodulation results at 66°C within 50 minutes.

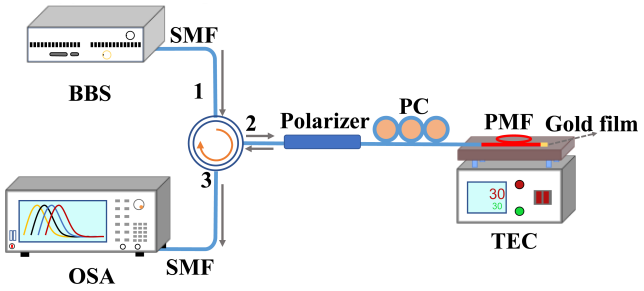

FIGURE 5. Experimental setup of the transmissive fiber Lyot filter for temperature measurement.

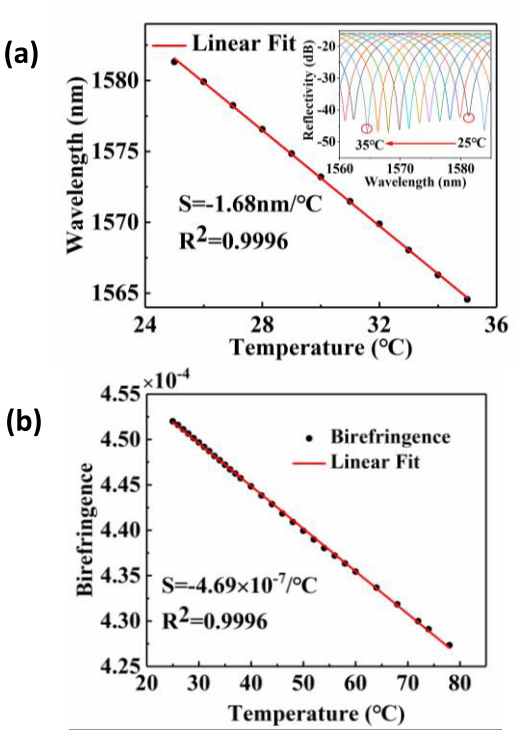

FIGURE 6. (a) The wavelength dip at 1581.3nm of the reflective spectrum shift versus temperature. Inset: Reflection spectrum response as temperature rise from 25°C to 35°C; (b) Birefringence of the reflective fiber Lyot filter versus temperature.

lead the BBS into the polarizer and transfer the reflection interference spectrum to the OSA. It should be noted that the PMF used in the reflective filter is only half the length of the transmissive type, which makes the sensor easy to be packaged. And the reflective structure can further expand the application range of the filter.

As shown in Fig. 6(a), the dip wavelength tracking method is first applied to the temperature measurement. The temperature sensitivity of -1.68nm/°C from the dip at 1581.3 nm is obtained, so according to Eq. 7, the corresponding birefringence sensitivity is about 4.7×10^{-7}/°C. And the inset shows the reflection spectra at different temperatures. Since the FSR of the spectrum is 18 nm, the measurement range of the sensor is limited to 25 −35°C. Furthermore, the interference spectrum is demodulated by the proposed least squares method, and the result is as shown in Fig. 6(b). We can see that the demodulation range of the temperature is 25 - 80 °C, which is 5.5 times more than the range demodulated by the dip wavelength tracking method. In addition, the birefringence sensitivity of the filter is 4.69×10^{-7}/°C, which is basically consistent with the sensitivity calculated. It should be pointed out that initial birefringence B of the reflective filter is slightly different from that of the transmissive filter at the same temperature. This may be because the measurement length of PMF is not completely accurate, resulting in a longer L_{PMF} in the model, which makes the B measured smaller. However, for a particular sensor, after the length is scaled, the sensitivity curve is determined and does not affect

the actual temperature measurement. Thanks to the high dip spectra are obtained in the experiments, the noises caused from the interference pattern are so low, which have little influence on the birefringence calculation of the Lyot filter.

IV. CONCLUSION

In conclusion, a birefringence demodulation method based on least squares algorithm has been proposed for expanding the temperature measurement range of the Lyot filter. We experimentally prepared two types of transmissive and reflective Lyot filters, both of which are demodulated by the dip wavelength tracking method and the least squares method. Experimental results show that the measurement range of the dip tracking method is limited by the FSR of the periodic interference spectrum, and the least squares demodulation can relatively enlarge the measurement range by at least 5.5 times. The proposed method not only utilizes high temperature sensitivity of the PMF, but also expands the temperature measurement range, which is of great significance for practical temperature measurement. It should be pointed out that by replacing the light source and receiver in the system with tunable lasers and photodetectors, combined with the proposed fitting method, low-cost automated temperature detection can be achieved. In addition, the method can be applied to other interference sensors that need to expand the measurement range.

REFERENCES

[1] M. Deng, L. G. Liu, Y. Zhao, G. L. Yin, and T. Zhu, "Highly sensitive temperature sensor based on an ultra-compact Mach–Zehnder interferometer with side-opened channels," *Opt. Lett.*, vol. 42, no. 18, pp. 3549–3552, 2017.
[2] Y. Xue, Y. S. Yu, R. Yang, C. Wang, C. Chen, J. C. Guo, X. Y. Zhang, C. C. Zhu, and H. B. Sun, "Ultrasensitive temperature sensor based on an isopropanol-sealed," *Opt. Microfiber Taper*, vol. 38, no. 8, pp. 1209–1211, 2013.
[3] S.-J. Qiu, Y. Chen, F. Xu, and Y.-Q. Lu, "Temperature sensor based on an isopropanol-sealed photonic crystal fiber in-line interferometer with enhanced refractive index sensitivity," *Opt. Lett.*, vol. 37, no. 5, pp. 863–865, 2012.
[4] L. Li, X. Li, Z. Xie, and D. Liu, "All-fiber Mach–Zehnder interferometers for sensing applications," *Opt. Express*, vol. 20, no. 10, pp. 11109–11120, May 2012.
[5] D. Wu, T. Zhu, K. S. Chiang, and M. Deng, "All single-mode fiber Mach–Zehnder interferometer based on two peanut-shape structures," *J. Lightw. Technol.*, vol. 30, no. 5, pp. 805–810, Mar. 1, 2012.
[6] X. Zhang, W. Peng, L.-Y. Shao, W. Pan, and L. Yan, "Strain and temperature discrimination by using temperature-independent FPI and FBG," *Sens. Actuators A, Phys.*, vol. 272, pp. 134–138, Apr. 2018.
[7] A. Urrutia, J. Goicoechea, A. L. Ricchiuti, D. Barrera, S. Sales, and F. J. Arregui, "Simultaneous measurement of humidity and temperature based on a partially coated optical fiber long period grating," *Sens. Actuators B, Chem.*, vol. 227, pp. 135–141, May 2016.
[8] Y. Wang, M. Yang, D. N. Wang, and C. R. Liao, "Selectively infiltrated photonic crystal fiber with ultrahigh temperature sensitivity," *IEEE Photon. Technol. Lett.*, vol. 23, no. 20, pp. 1520–1522, Oct. 15, 2011.
[9] Y. Yang, Y. Wang, Y. Zhao, J. Jiang, X. He, W. Yang, Z. Zhu, W. Gao, and L. Li, "Sensitivity-enhanced temperature sensor by hybrid cascaded configuration of a Sagnac loop and a F-P cavity," *Opt. Express*, vol. 25, no. 26, pp. 33290–33296, Dec. 2017.
[10] W. J. Ni, P. Lu, X. Fu, H. D. Sun, P. P. Shum, H. Liao, X. Y. Jiang, D. M. Liu, C. Y. Yang, J. S. Zhang, and Z. G. Lian, "Simultaneous implementation of enhanced resolution and large dynamic range for fiber temperature sensing based on different optical transmission mechanisms," *Opt. Express*, vol. 26, no. 14, pp. 18341–18350, Jul. 2018.
[11] B. Huang, X. Shu, Y. Wang, C. Mao, and Y. Wang, "Temperature- and strain-insensitive transverse load sensing based on optical fiber reflective Lyot filter," *Appl. Phys. Express*, vol. 12, no. 7, Jul. 2019, Art. no. 076501.
[12] O. Aharon and I. Abdulhalim, "Liquid crystal Lyot tunable filter with extended free spectral range," *Opt. Express*, vol. 17, no. 14, pp. 11426–11433, 2009.
[13] A. Gorman, D. W. Fletcher-Holmes, and A. R. Harvey, "Generalization of the Lyot filter and its application to snapshot spectral imaging," *Opt. Express*, vol. 18, no. 6, pp. 5602–5608, 2010.
[14] Z. Yan, C. Mou, H. Wang, K. Zhou, Y. Wang, W. Zhao, and L. Zhang, "All-fiber polarization interference filters based on 45°-tilted fiber gratings," *Opt. Lett.*, vol. 37, no. 3, pp. 353–355, 2012.
[15] Y. Li, J. Tian, M. Quan, and Y. Yao, "Tunable multiwavelength er-doped fiber laser with a two-stage Lyot filter," *IEEE Photon. Technol. Lett.*, vol. 29, no. 3, pp. 287–290, Feb. 1, 2017.
[16] K. Özgören and F. Ilday, "All-fiber all-normal dispersion laser with a fiber-based Lyot filter," *Opt. Lett.*, vol. 35, pp. 1296–1298, 2010.
[17] B. Huang and X. Shu, "Highly sensitive twist sensor based on Temperature- and strain-independent fiber Lyot filter," *J. Lightw. Technol.*, vol. 35, no. 10, pp. 2026–2031, May 15, 2017.
[18] X. Kang, W. Zhang, Y. Zhang, J. YANG, L. Chen, L. Kong, Y. Zhang, L. Yu, T. Yan, and P. Geng, "Intensity-demodulated torsion sensor based on thin-core polarization-maintaining fiber," *Appl. Opt.*, vol. 57, no. 13, pp. 3474–3478, 2018.
[19] Z. Yan, H. Wang, K. Zhou, Y. Wang, W. Zhao, and L. Zhang, "Broadband tunable all-fiber polarization interference filter based on 45° tilted fiber gratings," *J. Lightw. Technol.*, vol. 31, no. 1, pp. 94–98, Jan. 1, 2013.
[20] J. Zhang, X. Qiao, T. Guo, Y. Weng, R. Wang, Y. Ma, Q. Rong, M. Hu, and Z. Feng, "Highly sensitive temperature sensor using PANDA fiber Sagnac interferometer," *J. Lightw. Technol.*, vol. 29, no. 24, pp. 3640–3644, Dec. 15, 2011.
[21] D. Rife and R. Boorstyn, "Single tone parameter estimation from discrete-time observations," *IEEE Trans. Inf. Theory*, vol. 20, no. 5, pp. 591–598, Sep. 1974.
[22] Z. Xu and L. Zhao, "Key parameter extraction for fiber Brillouin distributed sensors based on the exact model," *Sensors*, vol. 18, no. 8, p. 2419, Jul. 2018.
[23] Y. Wu, L. Xia, N. Cai, and L. Zhu, "A highly precise demodulation method for fiber Fabry–Pérot cavity through spectrum reconstruction," *IEEE Photon. Technol. Lett.*, vol. 30, no. 5, pp. 435–438, Mar. 1, 2018.
[24] B. Huang, X. W. Shu, and Y. Q. Du, "Intensity modulated torsion sensor based on optical fiber reflective Lyot filter," *Opt. Express*, vol. 25, no. 5, pp. 5081–5090, 2017.

WEI LI received the Ph.D. degree in physical electronics jointly from the Huazhong University of Science and Technology (HUST), China, and the University of California at San Diego, San Diego, USA, in 2009. She is currently an Associate Professor with the School of Optical and Electronic Information, HUST. Her research interests include optoelectronic sensing and imaging, optical scattering theory, and fiber sensing technology.

TIANTIAN RUAN is currently pursuing the M.Eng. degree with the Huazhong University of Science and Technology. Her current research interests include the designing and testing of optical fiber sensors and demodulation techniques.

MIN XIA received B.Sc., M.Sc., and Ph.D. degrees in physical electronics from the Huazhong University of Science and Technology, Wuhan, China, in 2007. He is currently an Associate Professor with HUST. His research interests include optic fiber sensing and measurement, optical imaging, and machine learning.

LI XIA received the B.Sc., M.Sc., and Ph.D. degrees in electronic engineering from Tsinghua University, China, in 1994 and 2004, respectively. He is currently a Professor with the Huazhong University of Science and Technology, Wuhan, China. His research fields include the design and fabrication of passive fiber-based devices, optic sensing applications, and optical surface plasma resonance techniques.